

RESEARCH ARTICLE | JULY 03 2024

Dilutedly localized high-concentration ionogel electrolyte enabling high-voltage quasi-solid-state lithium metal batteries

Shufeng Song  ; Zongyuan Chen; Shengxian Wang; Fengkun Wei; Serguei V. Savilov ; Anji Reddy Polu ; Pramod K. Singh ; Zhaoqin Liu; Ning Hu

 Check for updates

Appl. Phys. Lett. 125, 013902 (2024)

<https://doi.org/10.1063/5.0221854>



Articles You May Be Interested In

Concentrated “ionogel-in-ceramic” and “ionogel-in-polymer” bilayer electrolyte membrane for high-voltage quasi-solid-state lithium metal batteries

Appl. Phys. Lett. (January 2024)

A hybrid solid electrolyte for high-energy solid-state sodium metal batteries

Appl. Phys. Lett. (June 2022)

Ion conduction and relaxation mechanism in ionogels embedded with imidazolium based ionic liquids

J. Appl. Phys. (October 2019)



Applied Physics Letters

Special Topics Open for Submissions

[Learn More](#)



Dilutely localized high-concentration ionogel electrolyte enabling high-voltage quasi-solid-state lithium metal batteries

Cite as: Appl. Phys. Lett. **125**, 013902 (2024); doi: [10.1063/5.0221854](https://doi.org/10.1063/5.0221854)

Submitted: 4 June 2024 · Accepted: 23 June 2024 ·

Published Online: 3 July 2024



View Online



Export Citation



CrossMark

Shufeng Song,^{1,2,a)}  Zongyuan Chen,² Shengxian Wang,² Fengkun Wei,² Serguei V. Savilov,³ 
Anji Reddy Polu,⁴  Pramod K. Singh,⁵  Zhaoqin Liu,¹ and Ning Hu⁶

AFFILIATIONS

¹Department of Aeronautical Mechanical and Electrical Engineering, Chongqing Aerospace Polytechnic, Chongqing 400021, China

²College of Aerospace Engineering, Chongqing University, Chongqing 400044, China

³Department of Physical Chemistry Engineering, M.V. Lomonosov Moscow State University, Moscow, Russia

⁴Department of Physics, BVRIT HYDERABAD College of Engineering for Women, Hyderabad 500090, Telangana, India

⁵Center for Solar Cells and Renewable Energy, Sharda University, School of Basic Sciences and Research, Greater Noida, Uttar Pradesh 201306, India

⁶State Key Laboratory of Reliability and Intelligence Electrical Equipment, National Engineering Research Center for Technological Innovation Method and Tool, and School of Mechanical Engineering, Hebei University of Technology, Tianjin 300401, China

^{a)} Author to whom correspondence must be addressed: sfsong@cqu.edu.cn

ABSTRACT

Ionogels, which are being considered as quasi-solid electrolytes for energy-storage devices, exhibited technical superiority in terms of non-flammability, negligible vapor pressure, remarkable thermostability, high ionic conductivity, and broad electrochemical stability window. However, their applications in lithium metal batteries (LMBs) have been hindered by several issues: poor compatibility with Li-metal anodes and high-voltage cathodes, high viscosity, and inadequate wettability. Little attention has been paid to ionogel-based low-concentration electrolytes, despite their potential advantages in terms of Li⁺ mobility, viscosity, electrode wettability, and cost. Here, we demonstrate the surprising capabilities of localized high-concentration ionogel (LHCI) and dilutely localized high-concentration ionogel (DLHCI) electrolytes, utilizing the non-solvating fluorinated ether 1,1,2,2-tetrafluoroethyl-2,2,3,3-tetrafluoropropyl ether, to realize high-voltage quasi-solid-state lithium metal batteries (QSLMBs). Notably, the DLHCI electrolyte not only delivers superior ionic conductivity of $3.93 \times 10^{-3} \text{ S cm}^{-1}$ but also provides a high Li plating/stripping Coulombic efficiency exceeding 99%. Moreover, it significantly enhances anodic stability when paired with 4.4 V LiNi_{0.8}Co_{0.1}Mn_{0.1}O₂ (NCM811) and 4.8 V LiNi_{0.5}Mn_{1.5}O₄ (LNMO). Consequently, substantial improvement in cycling performance of QSLMBs has been realized with the DLHCI electrolyte.

Published under an exclusive license by AIP Publishing. <https://doi.org/10.1063/5.0221854>

The current interest in ionogels, *viz.* ionic liquids (ILs) immobilized within solid scaffolds, is driven by their unique merits, including nonflammability, negligible vapor pressure, excellent thermostability, superior ionic conductivity, and broad electrochemical stability window.¹ These properties make ionogels a promising candidate for use as quasi-solid electrolytes in energy-storage devices. Researchers have investigated a great deal of inorganic and organic solid scaffolds for the confinement of various ILs to produce diverse ionogels with enhanced properties. Nevertheless, the Li plating and stripping in ionogel electrolytes have suffered from low current densities (typically around 0.1 mA cm⁻² and 0.1 mAh cm⁻²).²⁻⁴ In addition to the growth of Li dendrites,

another problem associated with the Li metal is the limited Li plating/stripping Coulombic efficiencies (CEs). The CEs in ionogel electrolytes, which reflect the loss of Li⁺ upon each cycle and serve as an indicator of the cycling stability of Li metal, have been scarcely reported in the literature. The available data show inferior CEs ranging from 19% to 94% in ILs.^{5,6} The diffusion of Li⁺ is faster through the bulk IL or the interfaces between scaffolds and IL but slower through the polymeric/inorganic scaffolds; consequently, the spatial nonuniformity of Li flux leads to the formation of Li dendrites.⁷ Furthermore, to maintain high ionic conductivities, ionogels generally contain minor proportions of solid scaffolds. However, this can weaken the diffusion of ILs and their

anions, leading to the side reactions and an unstable solid electrolyte interphase (SEI) on Li metal.

In addition to the challenges posed by Li-metal anodes, the lithium metal batteries (LMBs) with ionogel electrolytes have primarily realized Li plating/stripping in low-energy cathodes such as LiFePO₄ (LFP).^{8–10} This limitation arises from the restricted oxidative stabilization of ionogels and the formation of an unstable cathode electrolyte interphase (CEI) on cathodes. To maximize the specific energy of LMBs, a promising approach is to pair the Li metal with Ni-rich LiNi_xCo_yMn_{1-x-y}O₂ (NCM, $x > 0.6$) cathodes, such as LiNi_{0.8}Co_{0.1}Mn_{0.1}O₂ (NCM811). These cathodes offer high specific capacity, high voltage, and low price with less Co. However, increasing Ni content in the NCM cathodes, while enhancing the specific energy, also exacerbates dramatically the side reactions at electrolyte/cathode interfaces, leading to severe cycling failure.¹¹ Therefore, it is of great importance, yet remains challenge to regulate the ionogel electrolytes simultaneously stable to the Li-metal anodes and high-voltage Ni-rich cathodes.

Recently, we reported on a unique “superconcentrated ionogel-in-ceramic” electrolyte, prepared by enriching a garnet-type conductor with a superconcentrated ionogel (3 M LiTFSI–EmimFSI–PMMA). This electrolyte not only delivers superior Li⁺ conduction but also exhibits impressive stabilization for both Li-metal anode and LFP and NCM523 cathodes.¹² It has been energetically proposed that increasing salt concentration in solvents leads to a reduction in solvent molecules and alters solvation structure, thereby producing distinctive properties such as ion diffusion, interfacial stabilization, and electrochemical reversibility.¹³ The concept of high-concentration electrolyte (HCE, typically ≥ 3 M for Li salt concentration) is now widely recognized in the field of organic electrolyte.¹⁴ Specifically, several studies have shown salt-concentrated IL electrolytes can form stable interfaces with Li-/Na-metal anodes.^{15,16} However, these HCEs generally exhibit high viscosity, low Li⁺ mobility, and poor wetting on cathodes, limited capacity utilization and rate capability. Conversely, the localized high-concentration electrolytes (LHCEs, typically ≥ 1 –1.5 M for Li salt concentration) demonstrate favorable compatibility with Li-metal anodes, low viscosity, and good wettability.¹⁷ More recently, the low-concentration electrolytes (LCEs, typically < 1.0 M for Li salt concentration) have garnered significant interest due to their notable advantages in terms of cost and viscosity.¹⁸ These electrolyte chemistries have considerably broadened the research scopes of quasi-/solid-state electrolytes and serve as a valuable complement to the conventional liquid electrolytes (1–1.2 M of Li salt concentration). Despite this, the LCEs for high-voltage LMBs remain a significant challenges due to the uncontrollable decomposition of free solvents and the instability of the electrolyte/electrode interphases.^{19,20} While ionogel electrolytes provide prominent merits, they have received limited attention, especially in their low-concentration territory, despite the pressing issues surrounding them.

Here, we challenge this traditional wisdom and validate the extraordinary capabilities of the localized high-concentration ionogel (LHCI, 1.0 M) and the dilutedly localized high-concentration ionogel (DLHCI, 0.6 M) electrolytes to enable simultaneous stabilization toward Li-metal anode, 4.4 V NCM811 and 4.8 V LiNi_{0.5}Mn_{1.5}O₄ (LNMO) cathodes, and we realize enhanced cycling for high-voltage quasi-solid-state lithium metal batteries (QSLMBs).

Despite a few advancements in IL-/ionogel-based HCEs, the sluggish Li⁺ mobility and large viscosity of the ILs constrain the

performance of LMBs. Moreover, the “solidification” in ionogels further compounds these concerns. To tackle these issues, the non-solvating co-solvents, such as hydrofluoroethers or fluorinated aromatic compounds, have recently been used in IL electrolytes,²¹ inspired by organic-solvent-based LHCEs. Analogous to the organic-solvent-based LHCEs, the IL-based LHCEs exhibited typical Li salt concentration of 1–1.5 M.²² The strong electron-withdrawing effect of the fluorinated groups in non-solvating co-solvents reduces the solvating capability of the co-solvents toward Li⁺, thus produces more inert SEI layers.²³ Intriguingly, while significant research has been devoted to the organic-solvent-based and IL-based LHCEs, ionogel-based LHCEs have received limited attention. In this context, we have developed an ionogel-based LHCE (localized high-concentration ionogel, LHCI, 1.0 M). We have chosen a typical non-solvating fluorinated ether, 1,1,2,2-tetrafluoroethyl-2,2,3,3-tetrafluoropropyl ether (TTE), as it has been found to promote the formation of a stable SEI and enable the operation of high-voltage LMBs.¹⁷ By using the non-solvating TTE, the LHCI is anticipated to not only reduce the viscosity and enhance the Li⁺ mobility of ionogel but also strike a balance between the stability of electrolyte/electrode interfaces. Furthermore, we have expanded the LHCI concept to the dilutedly localized high-concentration ionogel (DLHCI, 0.6 M) electrolyte concept and demonstrate the superiority of DLHCI over LHCI in various electrochemical properties. To prepare the LHCI and DLHCI electrolytes, first, lithium bis(fluorosulfonyl)imide (LiFSI) was fully dissolved in N-methyl-N-propyl-pyrrolidinium bis(fluorosulfonyl)imide (Pyr₁₃FSI), and second, TTE was used to dilute the solution. Subsequently, methyl methacrylate (MMA) monomer, poly(ethylene glycol) dimethacrylate (PEGDMA) crosslinker, and azobisisobutyronitrile (AIBN) thermal initiator were added to the solution. Transparent and clear electrolytes can be obtained when the PMMA precursors were added. Last solidified electrolytes were received after thermally initiating radical polymerization at 60 °C [Fig. 1(a)]. As revealed by electrochemical impedance spectroscopy [Fig. 1(b)], the LHCI and DLHCI electrolytes showed ionic conductivities of 2.25×10^{-3} and 3.93×10^{-3} S cm⁻¹ at 25 °C, respectively, which are distinctly superior to those of the inorganic/organic ionogels and concentrated ionogels,^{1–4,12} indicating the considerably improved Li⁺ mobility. Meanwhile, negligible electronic conductivities of 1.46×10^{-9} and 2.45×10^{-9} S cm⁻¹ were observed in the LHCI and DLHCI electrolytes, respectively [Figs. 1(c) and S1]. The electrochemical stability of both electrolytes was determined by linear sweep voltammetry at 1 mV s⁻¹ scan rate between 2 and 7 V. Both the LHCI and DLHCI electrolytes exhibited similar anodic voltage limits of ~ 5.0 V vs Li/Li⁺ [Fig. 1(d)], indicating the fluorinated ether TTE would not weaken the resistance against oxidation. This wide voltage window provides a possibility of pairing Li-metal anode with high-voltage cathodes. Moreover, the DLHCI electrolyte showed Li⁺ transference number of 0.29 [Fig. 1(e)], slightly higher than that of LHCI (0.24) (Fig. S2). The Li⁺ transference number values were much higher than those of the IL-based LHCEs,^{22,23} which can be ascribed to the solidification of LHCI and DLHCI. Although both the DLHCI and LHCI electrolytes showed comparatively low Li⁺ transference number as compared with the solid polymer electrolytes, the further electrolyte chemistry design and regulation would strengthen the cation migration.

The Li|Cu cells with LHCI and DLHCI electrolytes were used to study the cycling stability of Li plating/stripping. The Li plating/

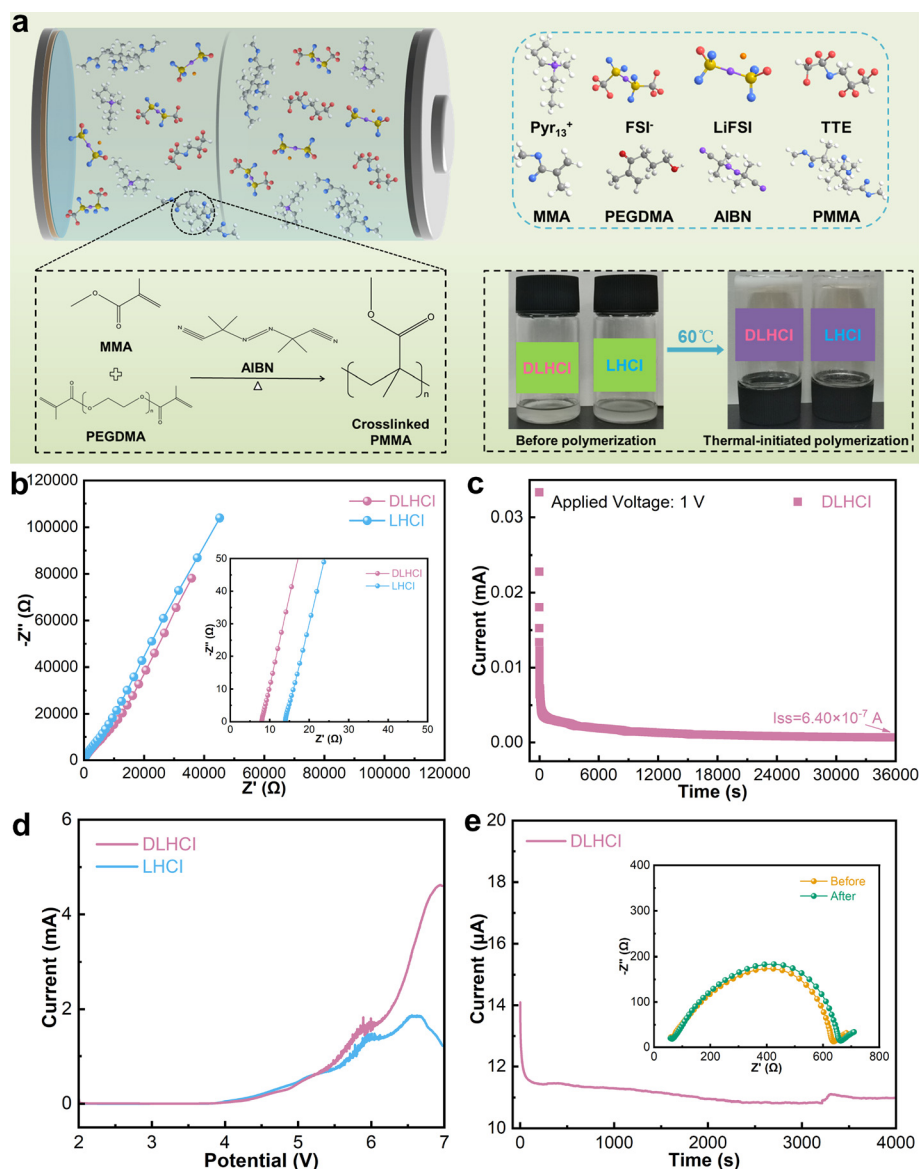


FIG. 1. (a) Schematic of the LHCI and DLHCI preparation. (b) Nyquist curves of LHCI and DLHCI electrolytes. (c) DC polarization curve of DLHCI. (d) Linear sweep voltammetry curves of LHCI and DLHCI. (e) Current-time profile of Li symmetric cell with DLHCI. The inset shows impedance spectra of the cell before and after polarization.

stripping CEs were determined according to the Aurbach's method.²⁴ A considerable discrepancy in the voltage profiles of the Li|Cu cells with different electrolytes was presented at 0.5 mA cm^{-2} [Fig. 2(a)]. Less Li can be stripped from the Cu electrode in the LHCI Li|Cu cell, implying that a few of plated Li on the Cu reacted with the LHCI electrolyte and cannot be reversible during the stripping process, whereas the DLHCI Li|Cu cell showed greater stripping capacity, demonstrating better interface stabilization. The Li electrodeposition in the DLHCI and LHCI electrolytes was compared with the nucleation overpotential, indicated by the voltage spike at the onset of Li electrodeposition. A higher nucleation overpotential (0.243 V for DLHCI compared to 0.229 V for LHCI) was observed [Fig. 2(b)]. The higher nucleation overpotential leads to the formation of more quantity of smaller nuclei on the electrode surface, thus generating uniform Li

electrodeposition.²⁵ In consequence, the DLHCI electrolyte provides a prominent Li CE of 99% at 0.5 mA cm^{-2} [Fig. 2(c)], and in sharp contrast, the LHCI electrolyte shows a moderate Li CE of 98%.

To further study the cycling stability of Li metal, symmetric Li|Li cells with both electrolytes were studied. Figure 2(d) shows the long-term cycling stability of the Li|Li cells with the LHCI and DLHCI electrolytes. Notably, the symmetric Li|Li cells were cycled for 500 h at a high current density of 1.0 mA cm^{-2} and a capacity of 1.0 mAh cm^{-2} . The DLHCI electrolyte exhibits stable and flat voltage profiles, accompanied by a stable overpotential. In contrast, the cycling of Li|Li cell with the LHCI electrolyte at this current density frequently exhibited increased voltage polarizations. Furthermore, Tafel curves and corresponding current density (Fig. S3) illustrate higher exchange current density (0.17 mA cm^{-2}) for the DLHCI, indicating better charge

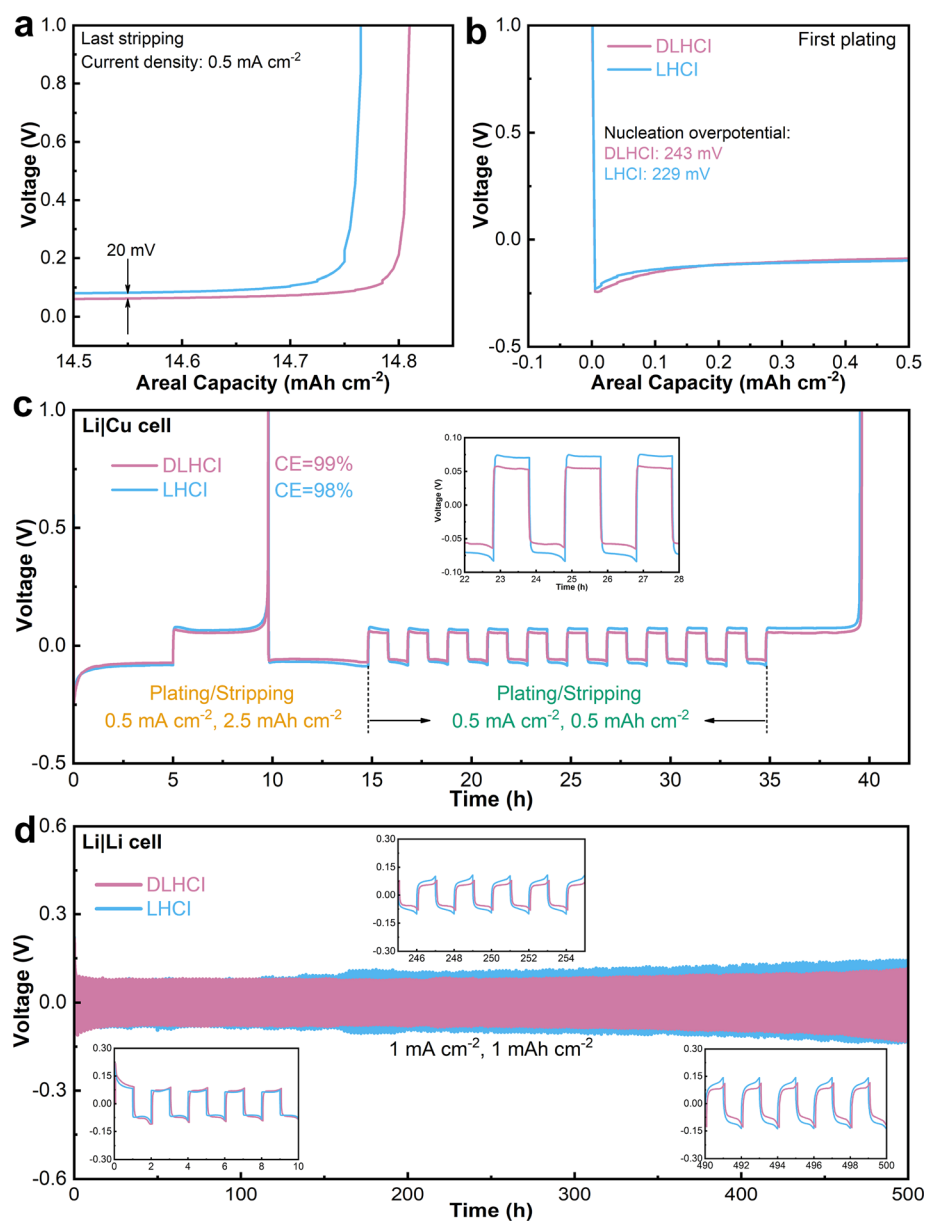


FIG. 2. (a)–(c) Voltage profiles from Li|Cu cells with LHCI and DLHCI. (d) Li plating/stripping in symmetric Li|Li cells with LHCI and DLHCI.

transfer capability. These findings validate the exceptional cycling stability of the DLHCI electrolyte, enabling the highly reversible plating/stripping of Li-metal anode even under high current density.

The use of LCEs for high-voltage LMBs has been hampered by severe decomposition of free solvents and the formation of unstable CEI layer. Consequently, despite their promise of delivering much higher specific energy, the LCEs have rarely been used in the high-voltage cathodes. To evaluate the resistance to anodic oxidation of the LHCI and DLHCI electrolytes, Li||NCM811 QSLMBs were fabricated and subjected to galvanostatic charging to a high cutoff voltage of 4.4 V at 0.5 C. Such condition pushed the electrolytes into a rather harsh oxidative test. The voltage decay was quite suppressed in the DLHCI electrolyte [Figs. 3(a) and 3(b)], indicating the suppression of

notorious structural transformation for the NCM811 from the layered to rock salt or spinel variants.²⁶ The DLHCI Li||NCM811 QSLMB delivers an initial discharge capacity of 177 mAh g^{-1} at 0.1 C [Fig. 3(c)], compared to 170 mAh g^{-1} of the LHCI QSLMB, indicating the high reversibility of NCM811 cathode with the DLHCI electrolyte. It is noted from Fig. 3(c) that the capacity of LHCI Li||NCM811 QSLMB has slightly sudden drop at about 140 cycles, which might ascribed to the oxidative decomposition of the LHCI electrolyte by the NCM811 cathode. Notably, the DLHCI Li||NCM811 QSLMB exhibits an acceptable capacity retention of 75% after 200 cycles at 0.5 C. In sharp contrast, continuous capacity decays and a moderate capacity retention of 43% were observed for the LHCI Li||NCM811 QSLMB [Fig. 3(c)]. This result reveals a significant improvement in the stability

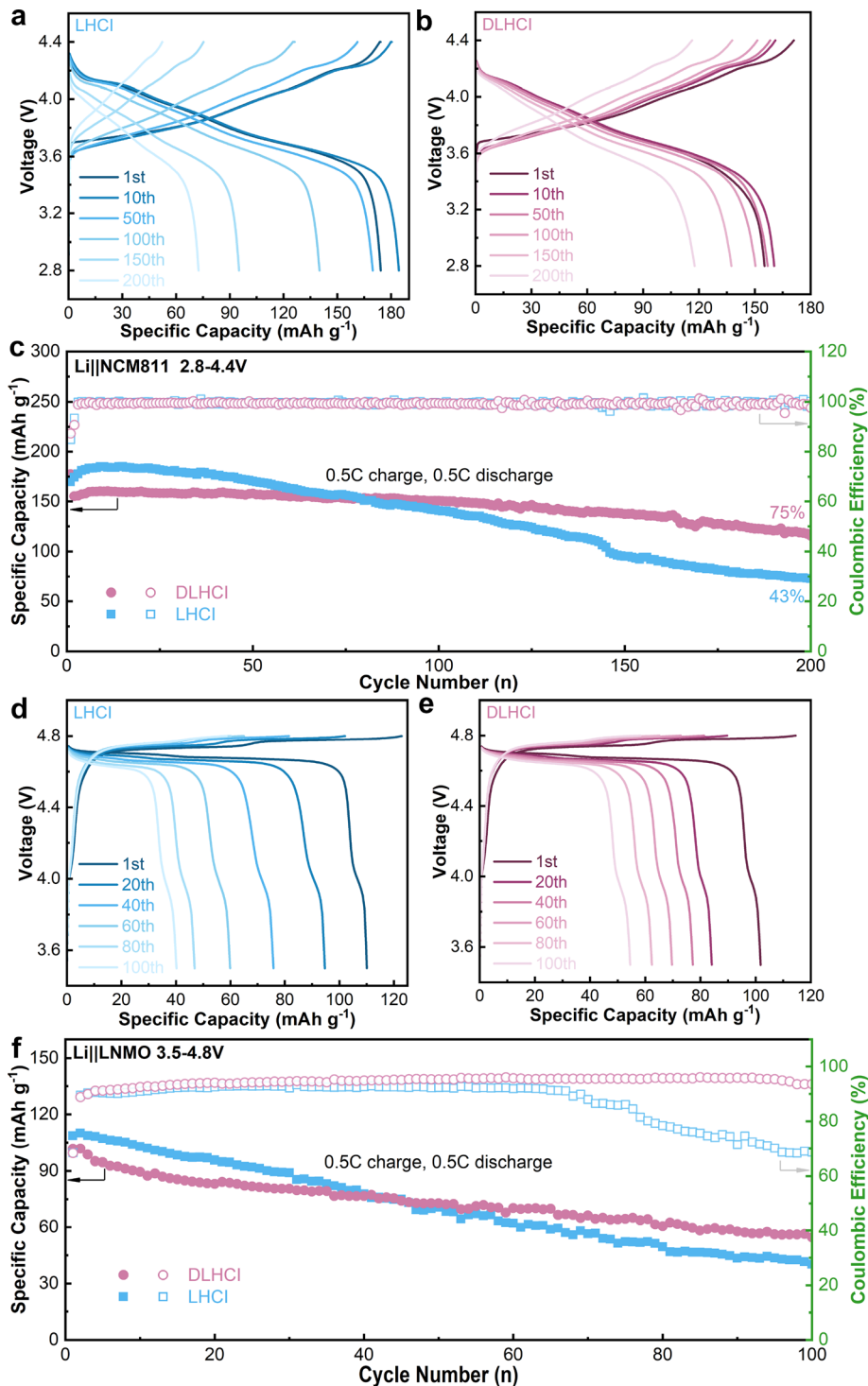


FIG. 3. Voltage–capacity profiles of Li||NCM811 QSLMBs with (a) LHCI and (b) DLHCI electrolyte. (c) Cycling performance of Li||NCM811 QSLMBs with LHCI and DLHCI. Voltage–capacity profiles of Li||LNMO QSLMBs with (d) LHCI and (e) DLHCI electrolyte. (f) Cycling performance of Li||LNMO QSLMBs with LHCI and DLHCI.

of LCEs toward the aggressive chemistry of both Li-metal anode and high-voltage cathode. To challenge the oxidative stability, we further assembled Li||LNMO QSLMBs with the LHCI and DLHCI electrolytes and charged to a very high cutoff voltage of 4.8 V at 0.5 C. Both the

Li||LNMO QSLMBs showed similar discharge capacity (102 mAh g⁻¹ for DLHCI compared to 109 mAh g⁻¹ for LHCI) [Figs. 3(d) and 3(e)]. However, the DLHCI Li||LNMO QSLMB offers a much higher capacity retention than the LHCI Li||LNMO QSLMB (54% compared to

TABLE I. Ionogel and low-concentration electrolytes comparison.

Study	Li metal		Cathode	Cycling Performance	Ref.
	Coulombic Efficiency	Symmetric Cells (mA cm ⁻² , mAh cm ⁻² , h)			
Biomimetic ant-nest SiO ₂ ionogel	None	0.1, 0.1, 600	LFP, NCM111	60 °C, 0.1 C, 10 cycles	27
Zwitterion-based copolymer ionogel	None	0.1, 0.05, 400	LFP	0.1 C, 200 cycles	28
Dual-layered ceramic-in-ionogel	None	0.1, 0.1, 1000	NCM811	0.1 C, 60 cycles	29
Layer-by-layer assembly ionogel	None	0.1, 0.3, 150	LFP	60 °C, 0.1 C, 80 cycles	30
Layered heterostructure ionogel	<18% and 98% for high-/low-potential ionogel	None	NCM111	0.1 C, four cycles	31
Zwitterionic surfactant-stabilized ionogel	None	0.1, 0.1, 600	LFP	0.5 C, 140 cycles	32
0.05M LiTFSI-0.05M LiPF ₆ -0.1M LiNO ₃ in DME:DIOX LCE	None	None	S	0.2 C, 200 cycles	33
0.3M LiFSI-0.2M LiTFSI in DX LCE	99.2%	0.5, 0.5, 150	LFP	0.5/1.0 C, 400 cycles	34
0.1M LiDFP-0.4M LBOB in EC:DMC LCE	97.6%	1.0, 1.0, 400	LFP	1.0 C, 300 cycles	35
0.05M LiTFSI-0.5M LiTFSI-0.2M LiNO ₃ in DME:DOL LCE	95%	1.0, 1.0, ~400	None	None	36
DLHCI	99%	1.0, 1.0, 500	NCM811	0.5 C, 200 cycles	Current work

37% after 100 cycles) [Fig. 3(f)]. At the elevated 0.5 C rate, the DLHCI Li||NCM811 and Li||LNMO QSLMBs deliver slightly lower initial discharge capacity as compared with the LHCI QSLMBs, which might be attributed to the low Li concentration in DLHCI. Exact mechanism is needed to be revealed in the further investigation. As a result, the DLHCI electrolyte was endowed a desirable capability of enabling high-voltage QSLMBs with underlying high specific energy and enhanced safety.

Our DLHCI electrolyte compares very observably against other favorable ionogel electrolytes and LCEs (Table I). The advanced ionogel electrolytes, which are typically associated with the inorganic nanomaterials and polymer skeletons, have primarily been evaluated in LFP battery structure, due to LFP's low operation voltage and stable structure. A few advanced ionogel electrolytes, such as those with layered heterostructure, have shown enhanced oxidative stability to enable high-voltage NCM battery structure, and their cycling performance remains limited. In addition, all these ionogel electrolytes have exhibited moderate Li plating/stripping at relatively low current densities of 0.1 mA cm⁻² in symmetric Li|Li cells. Furthermore, there is a lack of comprehensive evaluations on Li plating/stripping CE in diverse ionogel electrolytes. A recent study showed that a low CE (<18%) was observed with the high-potential ionogel electrolyte (1 M LiTFSI-EmimTFSI-BN), indicating intense reactions between the deposited lithium and ionogel at low potentials. Alternatively, a high CE (98%) was observed with the low-potential ionogel electrolyte (1 M LiTFSI-EmimFSI-BN).³¹ However, the low-potential ionogel electrolyte is unable to support the cycling of NCM111 battery. Overall, the ionogel electrolytes commonly exhibit moderate anodic stability and poor cathodic stability, which can be attributed to the weak efficiency of SEI and CEI stemmed from the ILs. Dai *et al.*³⁷ reported that, in comparison to a 5 M high-concentration IL electrolyte, the decomposition of LiFSI and the reduction of EmimFSI by Li metal were more significant in the standard 1.0 M IL electrolyte due to less effective SEI passivation.

Meanwhile, a uniform CEI layer (≈5–10 nm) was observed on the surface of NCM811 cathode after cycling in the high-concentration IL electrolyte. In contrast, an ultrathin (≈1 nm) and uneven CEI layer was formed in the standard 1.0 M IL electrolyte. On the other hand, the emerging LCEs create an opportunity to facilitate the interfacial charge transfer kinetics due to the weak solvation nature and demonstrated with the enhancement of the Li plating/stripping behavior and battery cycling. However, the low-voltage cathodes such as LFP and S were largely worked with the LCEs because the preferential organic-solvent decomposition in LCEs induces low interface stability. In particular, our DLHCI and LHCI electrolytes exhibit higher Li plating/stripping CEs and current densities. By moving the localized high-concentration ionogel to be more diluted, we overcome the relatively inferior interface instability arising from the IL, thus enable reversible cycling of high-voltage QSLMBs.

In summary, our research has unveiled an unanticipated capability of LHCI and DLHCI electrolytes, leveraging a non-solvating fluorinated ether, TTE, to realize high-voltage QSLMBs. The generation of DLHCI with a low Li-salt concentration of 0.6 M not only delivers desirable properties in regard to Li⁺ mobility, viscosity, electrode wettability, and cost but importantly also enables high stability against Li-metal anode and high-voltage cathodes simultaneously. Notably, utilizing the DLHCI electrolyte, we achieved a high Li plating/stripping CE exceeding 99% and were able to cycle a Li|Li cell at a high current density of 1.0 mA cm⁻² over 500 h. Furthermore, the Li||NCM811 QSLMB exhibited an enhanced capacity retention of 75% after 200 cycles at 0.5 C. Additionally, the Li||LNMO QSLMB demonstrated reversible cycling in DLHCI at a high cutoff voltage of 4.8 V. This study highlights the potential of diluted ionogel electrolytes in realizing high-energy and high-safety QSLMBs.

See the [supplementary material](#) for the preparation and characterization of the diluted localized high-concentration ionogel.

This work was supported by the Technical Innovation and Application Development Project of Chongqing (No. Z20230084), Key Program for International Science and Technology Cooperation Projects of the Ministry of Science and Technology of China (2021YFE0109700), the Chinese National Natural Science Fund (12227801 and 32300666), the Natural Science Foundation of Chongqing (cstc2021jcyj-msxmX0241 and cstb2023nscq-msx0303), Key Technologies and Demonstration Application Research Project for Large-scale Lithium-ion Hybrid Energy Storage Equipment (HC23118), and Hebei Province Military-civilian Integration Science and Technology Innovation Project (SJMYP2022X15).

AUTHOR DECLARATIONS

Conflict of Interest

The authors have no conflicts to disclose.

Author Contributions

Shufeng Song: Conceptualization (lead); Funding acquisition (equal); Methodology (lead); Project administration (equal); Resources (equal); Writing – original draft (lead); Writing – review & editing (lead). **Zongyuan Chen:** Data curation (lead); Formal analysis (lead); Methodology (equal); Software (lead); Validation (equal); Writing – original draft (supporting). **Shengxian Wang:** Data curation (equal); Formal analysis (equal); Validation (equal). **Fengkun Wei:** Data curation (equal); Formal analysis (equal); Validation (equal). **S. V. Savilov:** Formal analysis (supporting); Methodology (supporting). **Anji Reddy Polu:** Formal analysis (supporting); Methodology (supporting). **Pramod K. Singh:** Formal analysis (supporting); Methodology (supporting). **Zhaoqin Liu:** Formal analysis (supporting). **Ning Hu:** Formal analysis (supporting); Funding acquisition (equal); Project administration (equal); Resources (lead).

DATA AVAILABILITY

The data that support the findings of this study are available from the corresponding authors upon reasonable request.

REFERENCES

- J. L. Bideau, L. Viau, and A. Vioux, *Chem. Soc. Rev.* **40**, 907 (2011).
- L. Liang, X. Chen, W. Yuan, H. Chen, H. Liao, and Y. Zhang, *ACS Appl. Mater. Interfaces* **13**, 25410 (2021).
- X. Lin, S. Xu, Y. Tong, X. Liu, Z. Liu, P. Li, R. Liu, X. Feng, L. Shi, and Y. Ma, *Mater. Horiz.* **10**, 859 (2023).
- X. Song, C. Wang, J. Chen, S. Xin, D. Yuan, Y. Wang, K. Dong, L. Yang, G. Wang, H. Zhang, and S. Zhang, *Adv. Funct. Mater.* **32**, 2108706 (2022).
- J. K. Stark, Y. Ding, and P. A. Kohl, *J. Electrochem. Soc.* **158**, A1100 (2011).
- J. Fuller, R. Osteryoung, and R. Carlin, *J. Electrochem. Soc.* **142**, 3632 (1995).
- M. Liu, S. Zhang, E. R. H. van Eck, C. Wang, S. Ganapathy, and M. Wagemaker, *Nat. Nanotechnol.* **17**, 959 (2022).
- D. S. Ashby, R. H. DeBlock, C. H. Lai, C. S. Choi, and B. S. Dunn, *Joule* **1**, 344 (2017).
- C. M. Thomas, W. J. Hyun, H. C. Huang, D. Zeng, and M. C. Hersam, *ACS Energy Lett.* **7**, 1558 (2022).
- P. Guo, A. Su, Y. Wei, X. Liu, Y. Li, F. Guo, J. Li, Z. Hu, and J. Sun, *ACS Appl. Mater. Interfaces* **11**, 19413 (2019).
- X. Ren, L. Zou, X. Cao, M. H. Engelhard, W. Liu, S. D. Burton, H. Lee, C. Niu, B. E. Matthews, Z. Zhu, C. Wang, B. W. Arey, J. Xiao, J. Liu, J. G. Zhang, and W. Xu, *Joule* **3**, 1662 (2019).
- Y. Zhai, W. Hou, M. Tao, Z. Wang, Z. Chen, Z. Zeng, X. Liang, P. Paoprasert, Y. Yang, N. Hu, and S. Song, *Adv. Mater.* **34**, 2205560 (2022).
- Y. Yamada, J. H. Wang, S. Ko, E. Watanabe, and A. Yamada, *Nat. Energy* **4**, 269 (2019).
- M. Li, C. Wang, Z. Chen, K. Xu, and J. Lu, *Chem. Rev.* **120**, 6783 (2020).
- Y. Wang, C. J. Zanelotti, X. Wang, R. Kerr, L. Jin, W. H. Kan, T. J. Dingemans, M. Forsyth, and L. A. Madsen, *Nat. Mater.* **20**, 1255 (2021).
- D. A. Rakov, F. Chen, S. A. Ferdousi, H. Li, T. Pathirana, A. N. Simonov, P. C. Howlett, R. Atkin, and M. Forsyth, *Nat. Mater.* **19**, 1096 (2020).
- X. Ren, S. Chen, H. Lee, D. Mei, M. H. Engelhard, S. D. Burton, W. Zhao, J. Zheng, Q. Li, M. S. Ding, M. Schroeder, J. Alvarado, K. Xu, Y. S. Meng, J. Liu, J. G. Zhang, and W. Xu, *Chem* **4**, 1877 (2018).
- F. Wu, F. Chu, G. A. Ferrero, M. Sevilla, A. B. Fuertes, O. Borodin, Y. Yu, and G. Yushin, *Nano Lett.* **20**, 5391 (2020).
- Z. Jiang, Z. Zeng, H. Zhang, L. Yang, W. Hu, X. Liang, J. Feng, C. Yu, S. Cheng, and J. Xie, *iScience* **25**, 103490 (2022).
- Y. Quan, C. Gao, S. Wu, D. Zhao, J. Wang, C. Li, and S. Li, *New J. Chem.* **46**, 18498 (2022).
- S. Lee, K. Park, B. Koo, C. Park, M. Jang, H. Lee, and H. Lee, *Adv. Funct. Mater.* **30**, 2003132 (2020).
- X. Liu, A. Mariani, H. Adenusi, and S. Passerini, *Angew. Chem., Int. Ed.* **62**, e202219318 (2023).
- X. Liu, A. Mariani, T. Diemant, M. E. Di Pietro, X. Dong, M. Kuenzel, A. Mele, and S. Passerini, *Adv. Energy Mater.* **12**, 2200862 (2022).
- D. Aurbach, O. Youngman, Y. Gofer, and A. Meitav, *Electrochim. Acta* **35**, 625 (1990).
- P. Biswal, S. Stalin, A. Kludze, S. Choudhury, and L. A. Archer, *Nano Lett.* **19**, 8191 (2019).
- F. Schipper, H. Bouzaglo, M. Dixit, E. M. Erickson, T. Weigel, M. Talianker, J. Grinblat, L. Burstein, M. Schmidt, J. Lampert, C. Erk, B. Markovsky, D. T. Major, and D. Aurbach, *Adv. Energy Mater.* **8**, 1701682 (2018).
- N. Chen, Y. Dai, Y. Xing, L. Wang, C. Guo, R. Chen, S. Guo, and F. Wu, *Energy Environ. Sci.* **10**, 1660 (2017).
- J. Li, T. Zhang, X. Hui, R. Zhu, Q. Sun, X. Li, and L. Yin, *Adv. Sci.* **10**, 2300226 (2023).
- Q. Ruan, M. Yao, S. Luo, W. Zhang, C. J. Bae, Z. Wei, and H. Zhang, *Nano Energy* **113**, 108571 (2023).
- B. P. Thapaliya, I. Popov, and S. Dai, *ACS Appl. Energy Mater.* **3**, 1265 (2020).
- W. J. Hyun, C. M. Thomas, N. S. Luu, and M. C. Hersam, *Adv. Mater.* **33**, 2007864 (2021).
- J. H. Lee, J. C. Shin, J. Kim, J. W. Ho, W. J. Cho, M. J. Park, G. R. Yi, M. Lee, and P. J. Yoo, *J. Power Sources* **557**, 232565 (2023).
- R. Glaser, F. Wu, E. Register, M. Tolksdorf, B. Johnson, J. Ready, M. Sanghadasa, and G. Yushin, *J. Electrochem. Soc.* **167**, 100512 (2020).
- T. D. Pham, A. Bin Faheem, H. D. Nguyen, H. M. Oh, and K. K. Lee, *J. Mater. Chem. A* **10**, 12035 (2022).
- H. Zheng, H. Xiang, F. Jiang, Y. Liu, Y. Sun, X. Liang, Y. Feng, and Y. Yu, *Adv. Energy Mater.* **10**, 2001440 (2020).
- F. Chu, R. Deng, and F. Wu, *Energy Storage Mater.* **56**, 141 (2023).
- H. Sun, G. Zhu, Y. Zhu, M. C. Lin, H. Chen, Y. Y. Li, W. H. Hung, B. Zhou, X. Wang, Y. Bai, M. Gu, C. L. Huang, H. C. Tai, X. Xu, M. Angell, J. J. Shyue, and H. Dai, *Adv. Mater.* **32**, 2001741 (2020).